

Legends

Figure 1. *MiR-124* negatively regulates androgen receptor (AR). **A)** Western blot analysis of the AR expression in C4-2B CaP cells that were treated with 100 nM of synthetic *miR-124*, *miR-130*, *miR-384* or *miR-506*. The numbers under the gels are the fold changes of AR protein relative to untreated C4-2B cells (untreat.). Fold changes were calculated by scanning the AR bands and normalizing for β -actin bands. The upper portion is a schema of the first 436 bases of the AR 3' UTR (based on the RefSeq NM_000044.2). The digital numbers indicate the predicted three miRNA-binding sites targeted by six potential AR-targeting miRNAs. **B)** Western blot analysis of the expression of AR and PSA in LNCaP and C4-2B cells treated with 100 nM of *miR-124* mimic. Both mock and miRNA-NC were used as controls. **C)** Quantitative PCR (qPCR) assay of *miR-125b* levels in C4-2B and *cds2* cells treated with 100 nM of *miR-124* mimic or miR-NC. The values shown as mean \pm SE (n=3) are from three independent experiments performed in triplicate. **D)** Luciferase analysis in C4-2B cells. The assay was repeated three times with each assay being performed in four wells, and similar results were obtained each time. The representative results are shown as mean \pm SD (n = 4). The percentage represents enzyme activity in 100 nM *miR-124* mimic-transfected cells relative to that in 100 nM miR-NC-transfected cells. RLU, relative luciferase unit. Δ BS3'UTR, AR 3'UTR fragment lacking the *miR-124* binding site.

Figure 2. Quantitative PCR (qPCR) assays of *miR-124* expression levels in CaP cells. **A)** *MiR-124* abundance in two benign prostate cell lines (pRNS-1-1 and RWPE-1) and five CaP cell lines (22Rv1, LNCaP, LAPC-4, *cds2* and C4-2B). **B)** *MiR-124* expression levels in 19 benign prostatic hyperplasia (BPH) tissues, 44 primary CaPs, 6 lymph node metastases and 10 castration-resistant tumors. **C)** *MiR-124* levels in 18 matched benign and malignant prostate samples. The levels of *miR-124* of five pairs of prostate tissues (5, 8, 9, 11 & 16) were assayed using Northern blot analysis and similar results were obtained. The Northern blot results are shown in SI Figure 2B. “*”, no statistical difference (p>0.05) between BPH and CaP tissues.

In **A**, **B** and **C**, qPCR assays were repeated three times with each assay being performed in triplicate, and similar results were obtained each time. The values are shown as mean \pm SE (n=3).

Figure 3. The expression levels of androgen receptor (AR) and *miR-124* in four matched prostate tissues (pt-1 to pt-4). **A**) Immunohistochemical analysis of the AR protein in four human CaP samples (*right*) and their benign prostate tissue (*left*). **B**) qPCR detection of the abundance of *miR-124* in both BPH and CaP tissues. The values are shown as mean \pm SE from three independent experiments.

Figure 4. Methylation of *miR-124* in CaP cells. **A**) Expression levels of *miR-124* in 22Rv1, C4-2B and *cds2* CaP cell lines before and after treatment with 50 μ M of Aza. Results are expressed as fold change of *miR-124* relative to the untreated control. The assay was repeated three times with each assay being performed in three wells, and similar results were obtained each time. The representative results are shown as mean \pm SD (n = 3). **B**) Western blot analysis of the AR expression in LNCaP and C4-2B cells treated with 50 μ M of Aza. **C**) Methylation-specific PCR (MSP) assay of the 5' CpG islands of *miR-124-1*, *miR-124-2* and *miR-124-3* in seven prostatic cell lines: two benign lines (pRNS-1-1 and RWPE-1) and 5 malignant lines (22Rv1, LNCaP, LAPC-4, *cds2* and C4-2B). **D**) Bisulfite sequencing analysis of *miR-124* CpG island methylation in RWPE-1 cell line and five CaP cell lines. The top schematic view represents individual amplified 5' DNA fragments of three *miR-124* genes, which are located at -1895 to -1655 upstream of *pre-miR-124-1*, -1456 to -1188 of *pre-miR-124-2* and -1465 to -1246 of *pre-miR-124-3*. The vertical bars denote individual CpG dinucleotides. Methylation profiles of *miR-124* CpG island fragments in six cell lines tested were demonstrated in the bottom of the schema. CpGs are represented by open circles if unmethylated and by black circles if methylated. Each row exhibits methylated CpGs from at least three clones. The numbers on the right of each row are the percentage of methylated CpG dinucleotides. **E**) COBRA analysis of methylation of *miR-124-1*, *miR-124-2* and *miR-124-3* in 9 BPH tissues and 14 CaP samples. Purified PCR

product was digested with *Bst*UI that cuts methylated CGCG. The black arrows indicate the BPH samples having detectable methylation, and the white arrows indicate the CaP samples without methylation.

Figure 5. *MiR-124* induces apoptosis and upregulates p53. **A)** Annexin V assay of apoptosis. LNCaP and C4-2B cells were treated with 100 nM *miR-124* mimic or miR-NC for 4 days and stained with Annexin V and propidium iodide. Both early and late apoptotic cells are combined. The values are shown as mean \pm SE from three independent experiments. **B)** Western blotting analysis of p53 expression in 100 nM *miR-124* mimic-transfected C4-2B cells. Doxorubicin (Dox)-treated cells were used as positive control. **C)** Western blotting analysis of caspase 3 (Cas-3) in 100 nM *miR-124* mimic-transfected C4-2B cells. In both **B** and **C**, the numbers under the gels are the fold changes of p53 and Cas-3 in *miR-124* mimic-treated C4-2B cells relative to miR-NC-treated cells.

Figure 6. Inhibition of xenograft tumor growth by *miR-124*. **A)** Five nude mice per group were injected subcutaneously with 2×10^6 22Rv1-*miR-124* cells, 22Rv1-vector cells, or untreated 22Rv1 cells. The growth of xenograft tumors were measured twice per week. Each time point represents mean \pm SD of five independent values (mm^3). **B)** qPCR assay of *miR-124* level in xenograft tumors. The assay was repeated twice and similar results were obtained each time. The representative results are shown as mean \pm SD (n = 3). **C)** Western blot assay of the AR expression in two 22Rv1-*miR-124* tumors that express the full-length AR and a truncated AR (Tepper et al 2002).

Type of file: figure

Label: Figures including supplementary figures

Filename: Oncogene All Figures.pdf

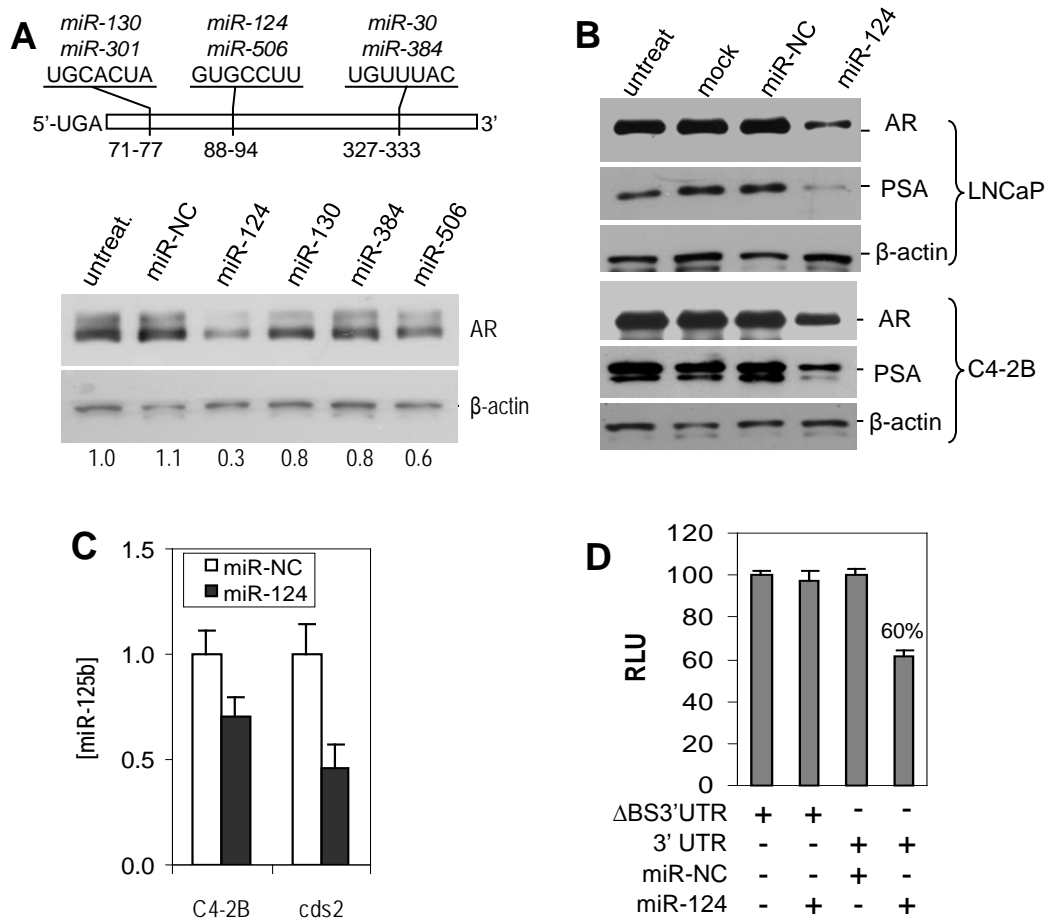


Fig. 1

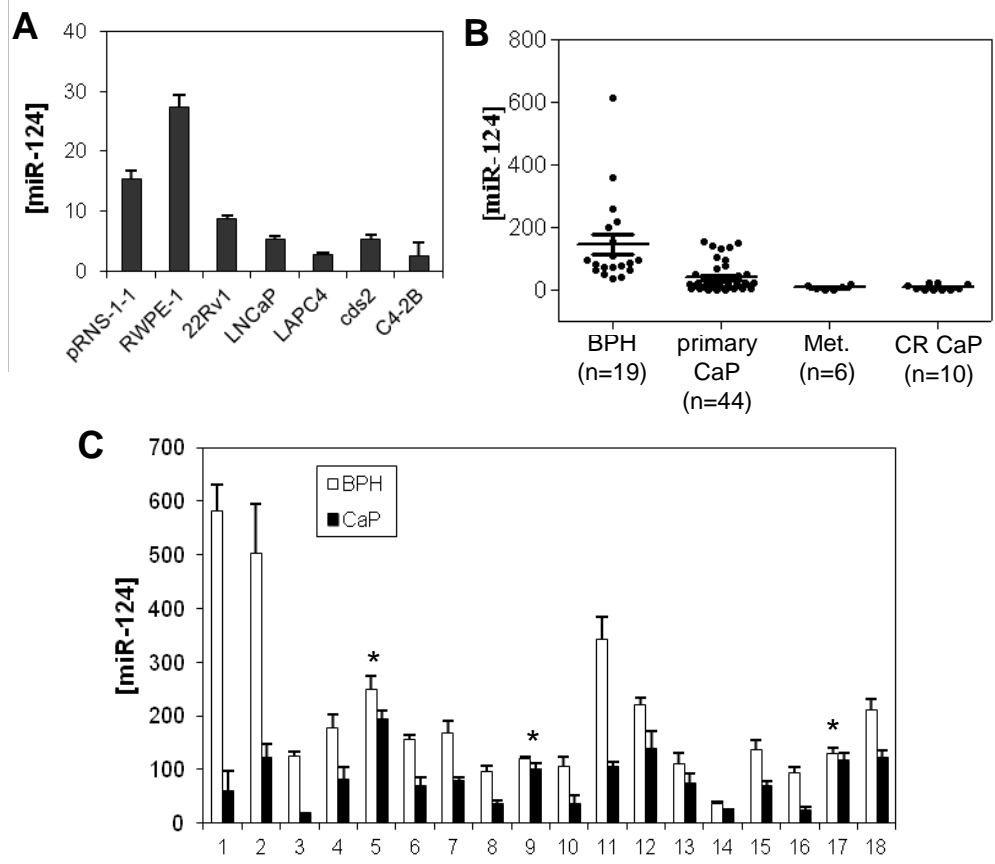


Fig. 2

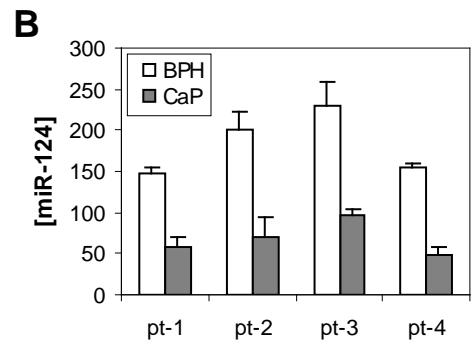
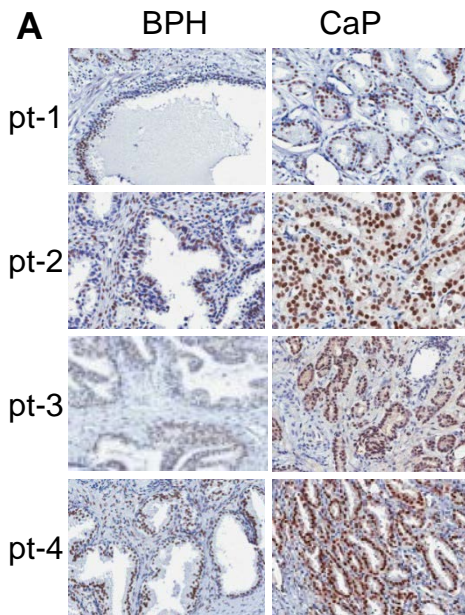


Fig. 3

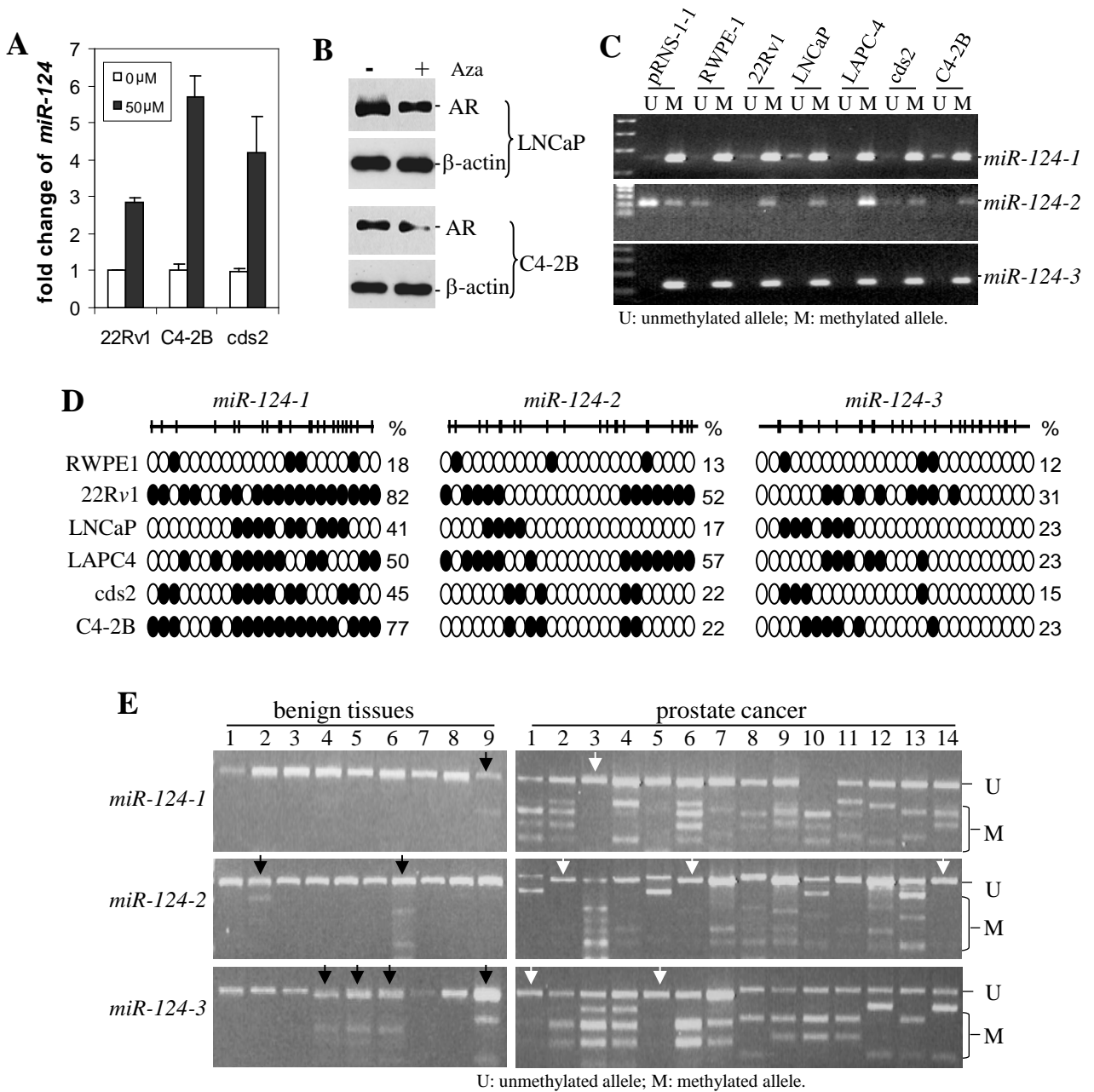


Fig. 4

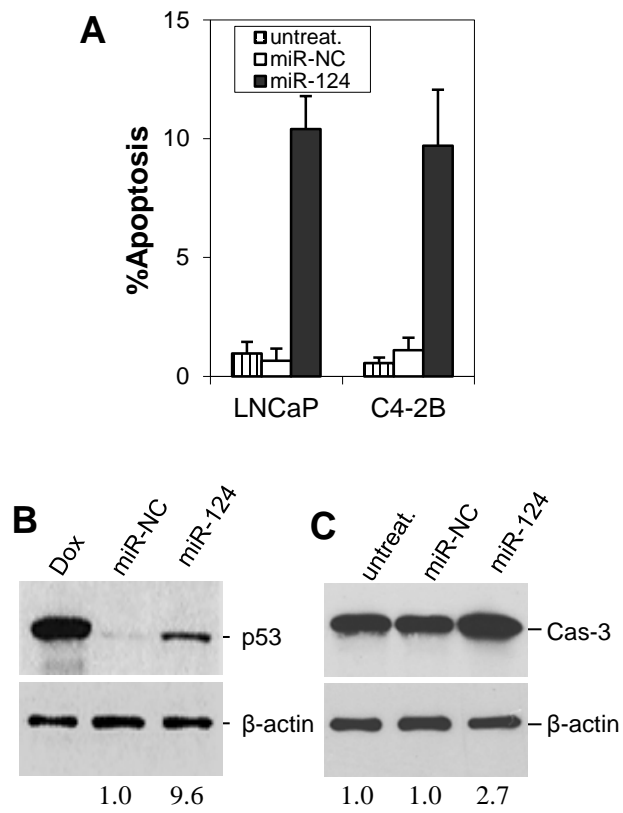


Fig. 5

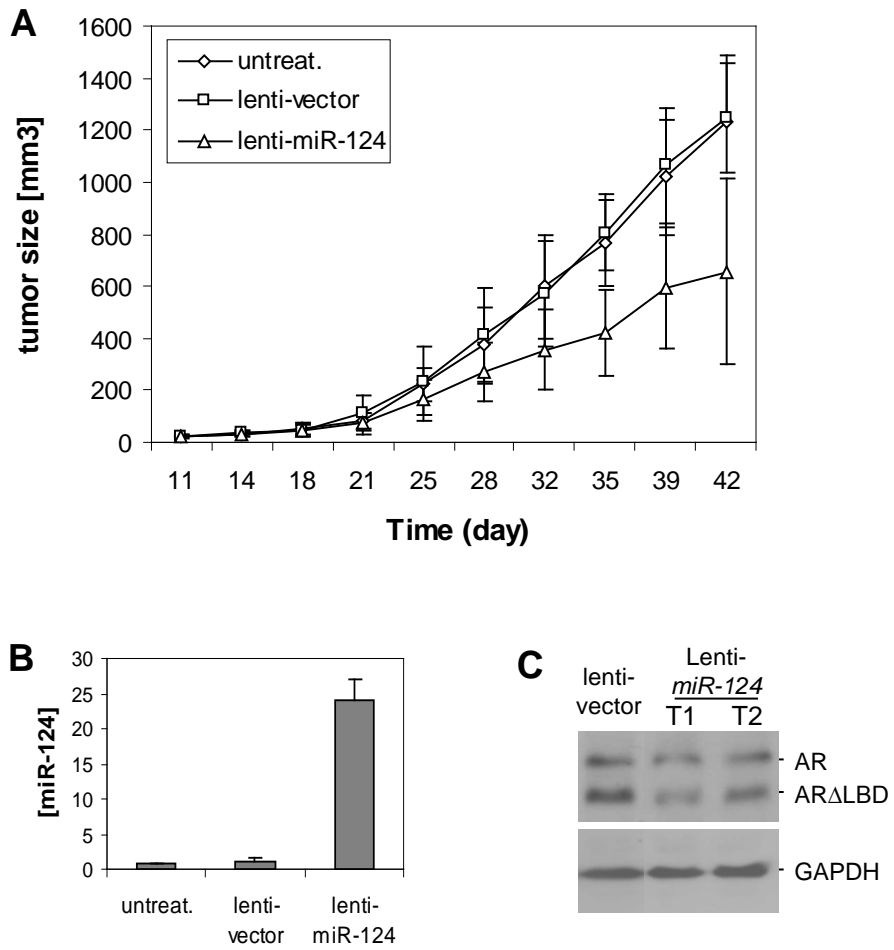
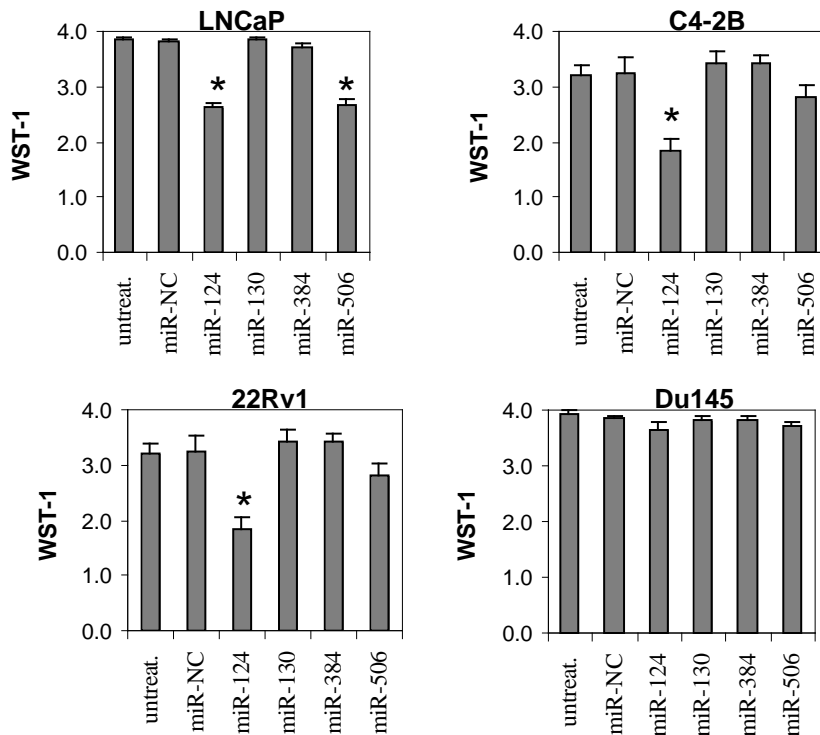
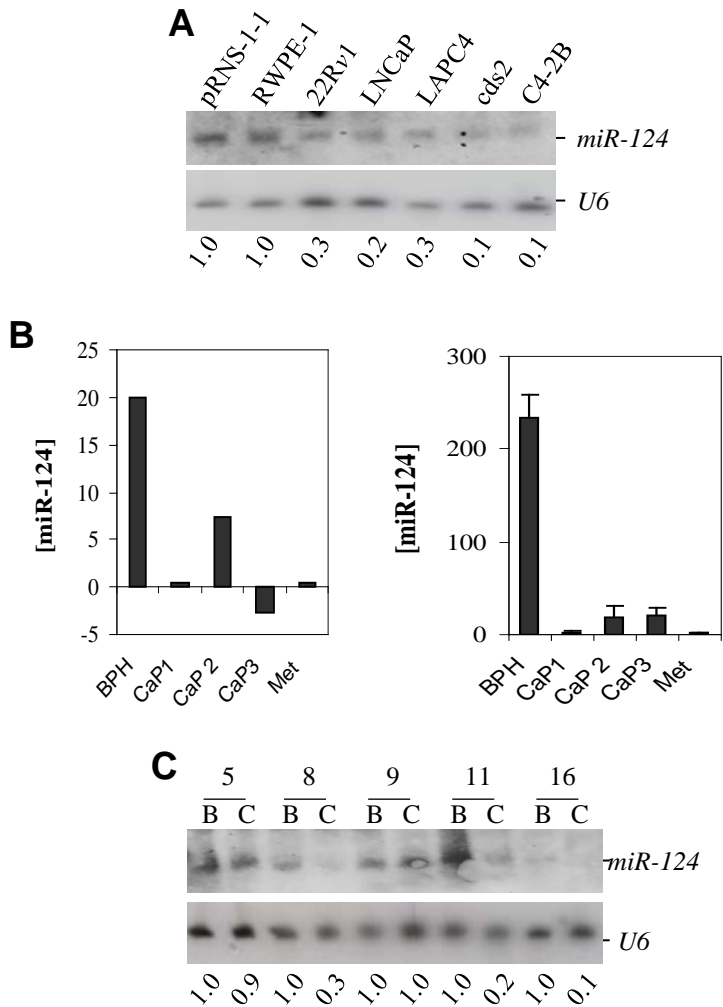


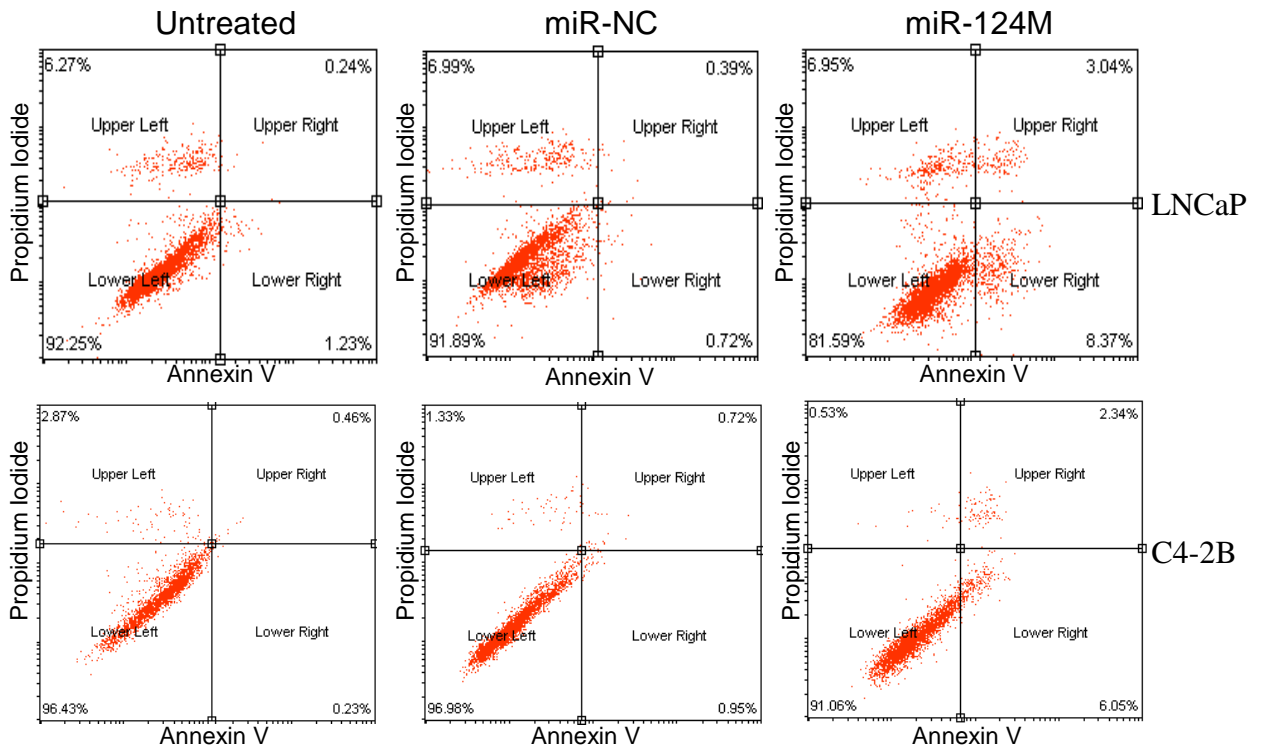
Fig. 6



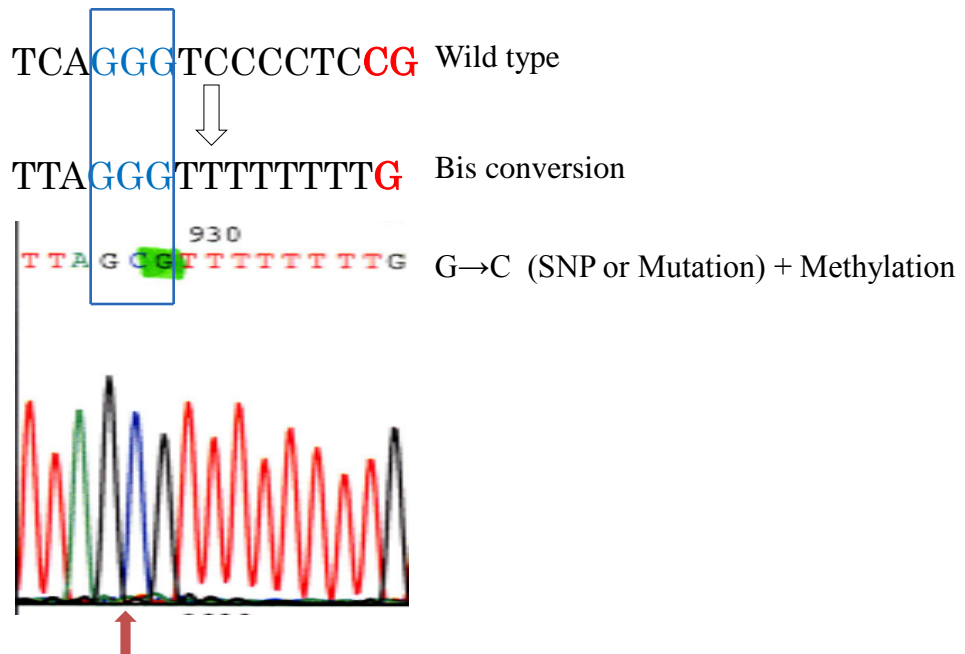
SI Figure 1. *miR-124* inhibits the proliferation of CaP cells. WST-1 cell proliferation analysis of AR-positive CaP cell lines. Cells (4×10^3 per well) were plated in 96-well plates for 24 hours, and then transfected with 100 nM synthetic miRNA mimics (miR-124m, miR-130m, miR-384m or miR-506m) or miRNA negative control (miR-NC) using lipofectamine 2000 (Invitrogen). The transfection protocol was optimized using a fluorescent pEGFP-N1 vector (Clontech) to ensure a transfection efficiency >90%. WST-1 cell proliferation assay was carried out at Day 5 after transfection. The growth changes were demonstrated as $M \pm SD$ ($n = 3$). AR-negative DU-145 cells were used as control that shows a slight inhibition of proliferation caused by miRNA mimics. “*” indicates a significant difference ($p < 0.05$) relative to miR-NC.



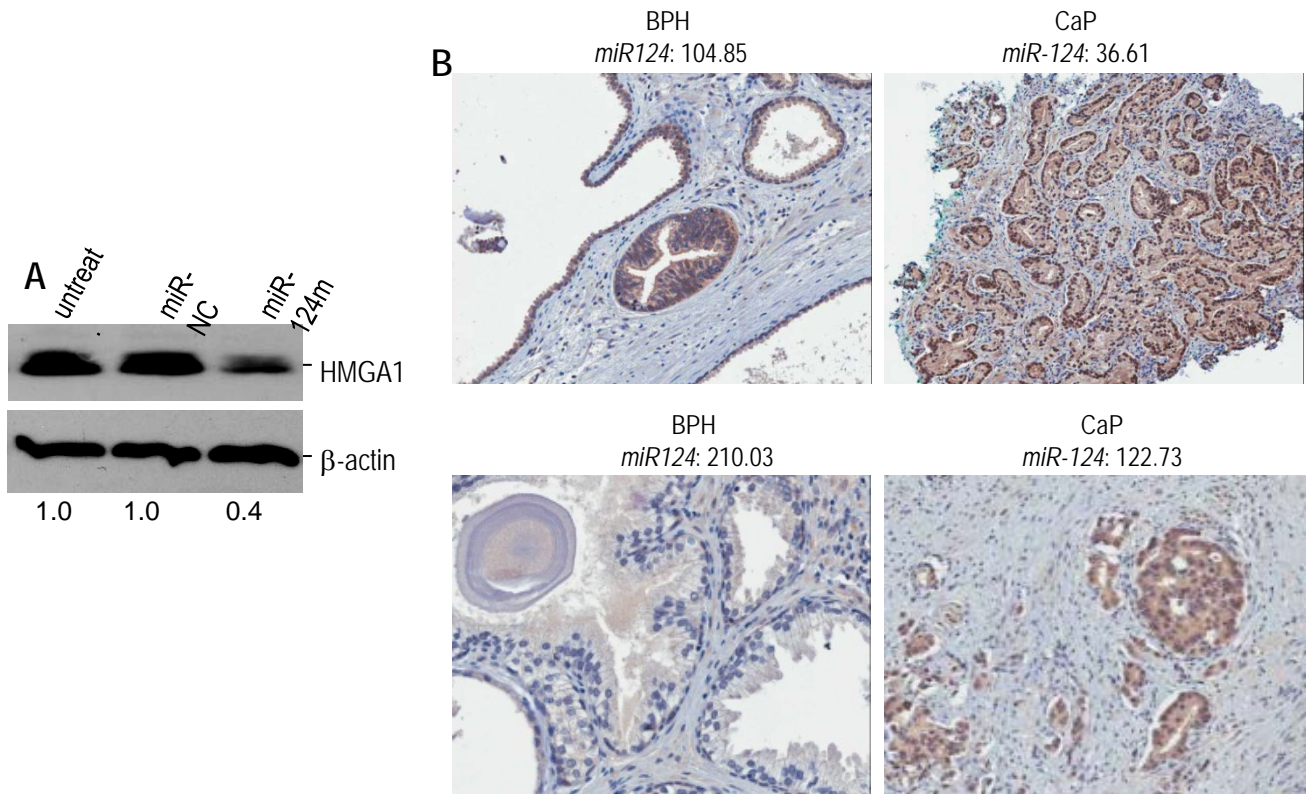
SI Figure 2. Downregulation of *miR-124* in CaP cell lines and in clinical specimens. **A)** To validate the qPCR results shown in Figure 2A, Northern blot assay was performed for *miR-124* expression in seven prostate cell lines (two benign and five malignant). The *miR-124* expression pattern is similar to that observed in qPCR. The numbers under the gel are the fold changes of *miR-124* in CaP cells (22Rv1, LNCaP, LAPC4, cds2 and C4-2B) relative to in benign cells (pRNS-1-1 and RWPE-1). **B)** The expression levels of *miR-124* in one BPH and four CaP tissues (including a lymph node metastasis, Met) was summarized from a previous microarray profiling assay (*left*). The *miR-124* levels detected in the microarray profiling were validated by qPCR (*right*). **C)** Northern blot assay for *miR-124* in five CaP specimens that have sufficient amount of RNA. Three CaP samples (8, 11 and 16) having low *miR-124* levels detected by qPCR exhibit lower signal intensity in North blots, compared to their BPH matches. Two CaP samples (5 and 9) and their BPH matches exhibit similar signal intensity in North blots. The numbers under the gel are the fold changes of *miR-124* in CaP cells relative to in benign cells. B, BPH; C, CaP. *U6* was used as loading control.



SI Figure 3. LNCaP (*top*) and C4-2B (*bottom*) cells transfected with 100 nM of miR-124m or miR-NC were grown in 10% FBS medium for four days. Both early apoptosis and later apoptosis were analyzed using Annexin V apoptosis assay protocol.



SI Figure 4. A point mutation or single nucleotide polymorphism (SNP) was detected at the 5' CpG region (1267 upstream of pre-miR-124-2) in a clinical CaP specimen. The wild-type “G” changed to “C” and was methylated (pointed out by an arrow).



SI Figure 5. Analyses of the expression of HMGA1 in CaP cells. *A*) Western blotting analysis of HMGA1 expression in 100 nM miR-124m-transfected C4-2B cells. The numbers under the gels are the fold changes of HMGA1 in miR-124m-treated C4-2B cells relative to miR-NC-treated cells. Our pilot results indicate that miR-124m treatment induced the downregulation of HMGA1 by ~60%. *B*) Immunohistochemical analysis of the expression of HMGA1 in two matched BPH and CaP tissues. CaP samples (*right*) and their BPHs (*left*) were immunostained using anti-HMGA1 antibody (sc-26348, Santa Cruz Biotechnology, Inc.). The abundance of *miR-124* in these tissues was measured using qPCR, and the values are shown on the top of each image. CaP tissues express lower level of *miR-124* than BPHs. Immunostaining for HMGA1 is more intense in two CaP samples than that in BPH matches. Moreover, localization of HMGA1 in the cytoplasm of CaP cells was obvious compared to that in BPH cells.